EUROPEAN CONFERENCE ON INTEGRATED OPTICS

Performance tradeoffs in low-loss Si_3N_4 waveguides for linear and nonlinear applications

(Student paper)

Marcello Girardi[1*], Anders Larsson[1], and Victor Torres-Company[1]

[1]Department of Microtechnology and Nanoscience, Chalmers University of Technology, SE-41296, Sweden
[*] girardi@chalmers.se

We experimentally analyze tradeoffs in terms of waveguide losses, dispersion engineering and single-mode behaviour for different waveguide geometries. Our results suggests that photonic integrated circuits relying on nonlinear waveguides benefit from including a dedicated waveguide geometry via multi-layer integration to yield a seven-fold improvement in terms of loss.

Keywords: *silicon nitride, waveguide, nonlinear, low-loss, photonic integrated circuits*

INTRODUCTION

Silicon nitride (Si_3N_4) is a versatile material platform for photonic integration thanks to its wide transparency window, strong Kerr nonlinearity, high refractive index, and absence of two-photon absorption [1], [2]. This allowed the development of waveguides with ultralow loss, in the order of 1dB/m or lower [2]–[4], which proved to be crucial for Si_3N_4-based nonlinear optics applications, e.g., frequency comb generation [5] and generation of squeezed quantum states [6]. Nonlinear applications require a careful design of the waveguide geometry to attain the desired dispersion. These waveguides feature strong confinement but unfortunately are multimode (MM), which represents a potential problem when assembled together with other linear components to build complex photonic integrated circuits, e.g., in programmable photonic circuits [7] and quantum photonics [6].

Linear optics requires a single-mode (SM)-waveguide design to avoid parasitic coupling to higher order modes [8]. Starting from a dispersion-engineered strong-confinement design, the only way to achieve SM operation in Si_3N_4 is to reduce the waveguide width. However, this results in a mode with stronger interaction with the sidewalls and increased radiation loss due to roughness [9]. As a result, there is a fundamental tradeoff between single-mode behaviour, dispersion-engineering and losses in strong-confinement Si_3N_4 waveguides.

Advances in multi-layer integration [10] would allow bridging between Si_3N_4 layers featuring different thicknesses, hence effectively overcoming the aforementioned tradeoff. One could envision e.g. to attain dispersion-engineered nonlinear waveguides in a thick Si_3N_4-layer featuring strong optical field confinement and with the aid of interposers, enable an adiabatic transition to a low-confinement waveguide geometry with SM operation for linear processing [11], [12]. Before resorting to implement such a dual-layer platform, it is crucial to evaluate quantitatively the potential gains in improved losses. That is exactly the objective of this work. Here we present the

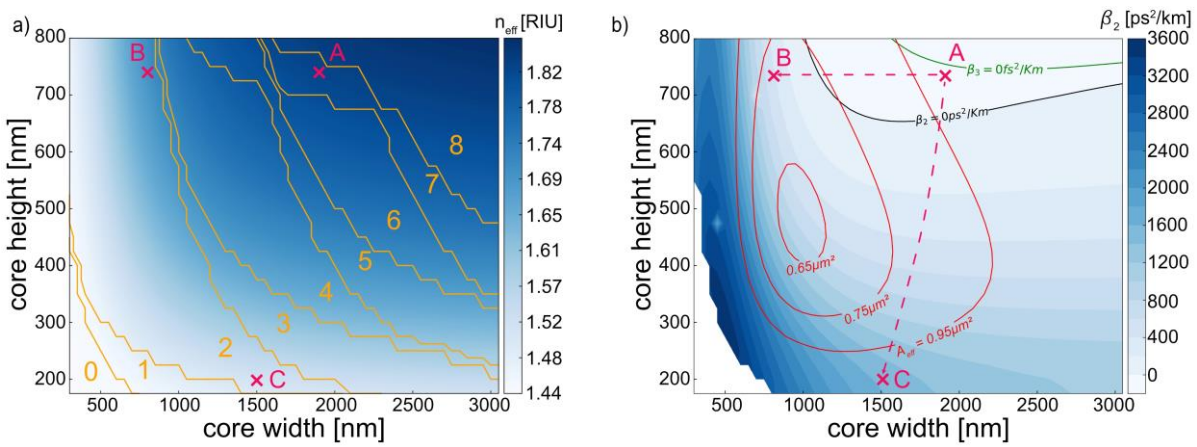

Fig. 1. a) Effective refractive index of the fundamental TE mode and number guided modes (orange lines). b) Color map of the dispersion (β_2) with the zero-dispersion line (black), the zero third order dispersion line (green) and the effective area (A_{eff}) of the fundamental TE mode (red). The magenta crosses represent the three geometries tested and the arrows show the two strategies considered to attain single mode operation.

first comprehensive experimental analysis of the trade-offs in optical losses between using a dispersion-engineered platform and a dedicated platform for single-mode operation. A crucial aspect of this analysis is that the assessment is done with minimum changes in the etching process, thus allowing for a meaningful and fair comparison between waveguide geometries.

RESULTS

The three waveguide geometries selected for this study are a dispersion-engineered waveguide with thickness 740nm and width 1900nm (A), a SM waveguide 800nm wide with the same thickness (B), and a SM waveguide with reduced thickness, i.e. 200nm thick and 1500nm wide (C). The three geometries are represented by the magenta crosses in figure 1a. The dispersion-engineered waveguide geometry was selected to attain anomalous dispersion and a third-order dispersion coefficient close to zero (see figure 1b). These parameters are crucial to the generation of Kerr soliton frequency combs but, as showed in figure 1a, the waveguide supports six modes, three in the TE and three in the TM polarization. From figure 1a, one can observe that pure SM operation is not possible with a thickness of 740nm, but a waveguide with width <850nm is SM with two supported polarizations, hence our choice of the second waveguide geometry B. In figure 1b we can see that in this condition the mode effective area (A_{eff}) is small, i.e., the interaction with the sidewalls is strong. To decrease the interaction with the sidewalls, we opted for a larger A_{eff}, maintaining the SM condition, i.e., the thin waveguide geometry C. Moreover, this geometry maintains a simulated critical bending radius of ~100µm, as showed in figure 2f. This allows the development of more compact devices compared to ultrathin waveguides, which feature a critical bending radius ten times larger [3].

To test the three geometries, we fabricated two different samples, one for each thickness. The samples were fabricated on 100mm wafers with a subtractive fabrication approach. The 740nm thick sample followed the fabrication flow reported in our previous work [13]. The fabrication of the 200nm thick sample followed a simplified processing since stress release trenches are not necessary for this thickness. As shown in the SEM pictures reported in figure 2d and 2e, the fabrication process yields waveguides with ultra-smooth sidewalls, believed to be in the sub nm scale, i.e. below the resolution of our SEM.

To evaluate the loss of the waveguides we designed ring resonators with point coupling and bending radius of 227µm. The bending radius was selected to minimize the bending loss and achieve an FSR of ~100GHz. The rings were characterized via sweep wavelength interferometry in the range 1500-1600nm following the procedure described in [14]. From the measurement, we obtained the intrinsic linewidth of the cavities (k_0). The histograms

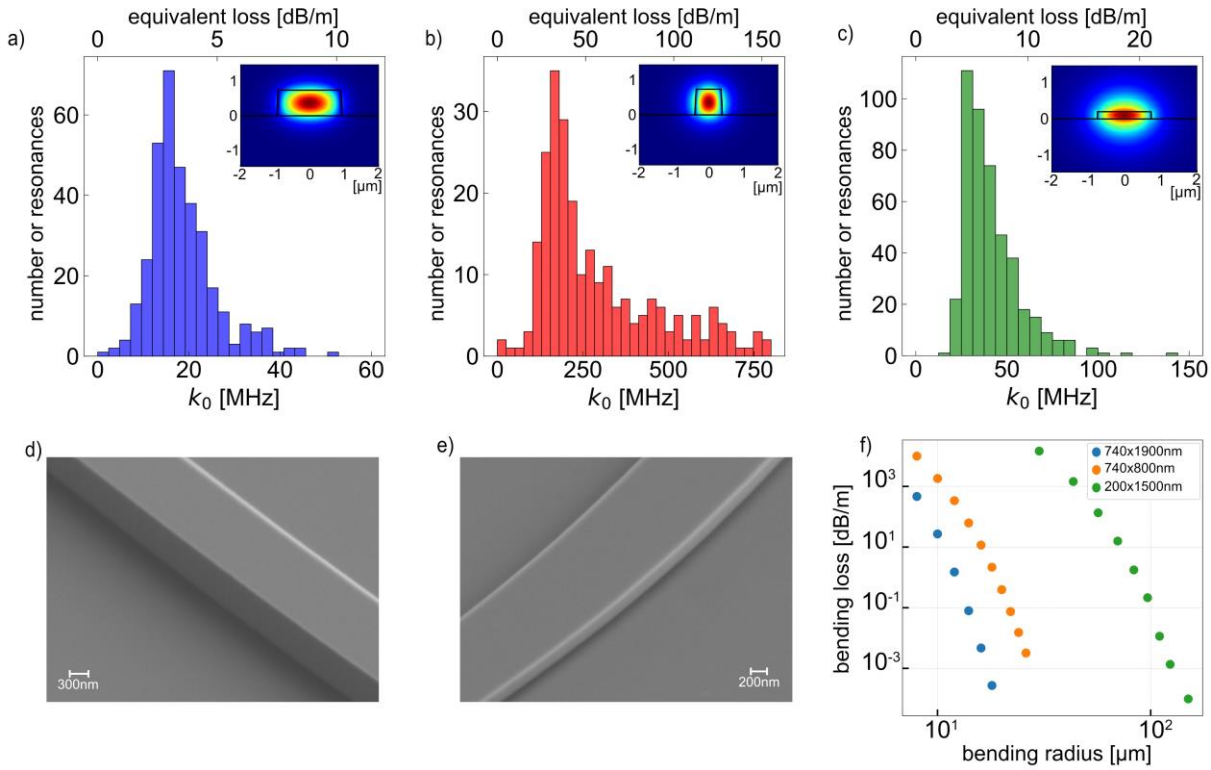

Fig. 2. a), b), c) Histograms of the intrinsic linewidths and equivalent propagation loss measured for the three different geometries, respectively (A) 740x1900nm, (B) 740x800nm and (C) 200x1500nm and mode field distributions (insets). d), e) SEM picture of the 740x800nm and 200x1500nm waveguides in tilted view to show the sidewalls. f) Simulated bending loss for the three geometries considered.

of k_0 for the three different geometries are reported in figure 2a, 2b and 2c, with the equivalent propagation loss on the upper axis. As expected, increasing the confinement factor from a multimode to a single mode waveguide, without changing the thickness leads to an increase of the equivalent propagation loss. The most probable value raises from 2.7 dB/m of the multimode waveguide (A) to 30.0 dB/m of the single mode waveguide (B). This is explained by the stronger interaction of the mode with the sidewalls [15], as clearly showed by the smaller A_{eff} in figure 1b, and the mode field distribution in the inset of figure 2b. The most probable equivalent propagation loss for the thin Si_3N_4 geometry (C) is 4.1 dB/m which is a more than a seven-fold improvement of the propagation loss for single mode application. This type of geometry will prove beneficial in large devices, e.g., arrayed waveguide grating multiplexers or long delay lines, where it is paramount to avoid modal dispersion and long propagation length are necessary.

CONCLUSION

We experimentally benchmarked in terms of losses two different waveguide thicknesses to show the trade-off for SM operation. We demonstrated that a thinner SM waveguide with moderate confinement has seven times better loss compared to a strong confinement SM waveguide. This suggests that integrating multiple dedicated platforms via 3D integration will be beneficial for complex photonic integrated circuits, e.g., quantum photonic circuits.

Acknowledgements: This work was performed in part at Myfab Chalmers. We acknowledge suport from the European Research Council (GA 771410) and the Swedish Research Council (2016-06077 and 2020-00453).

References

[1] P. Muñoz *et al.*, “Silicon nitride photonic integration platforms for visible, near-infrared and mid-infrared applications,” *Sensors (Switzerland)*, vol. 17, no. 9, p. 2088, 2017.

[2] J. Liu *et al.*, “High-yield, wafer-scale fabrication of ultralow-loss, dispersion-engineered silicon nitride photonic circuits,” *Nat. Commun.*, vol. 12, 2021.

[3] M. W. Puckett *et al.*, “422 Million intrinsic quality factor planar integrated all-waveguide resonator with sub-MHz linewidth,” *Nat. Commun.*, vol. 12, 2021.

[4] Z. Ye, P. Zhao, K. Twayana, M. Karlsson, V. Torres-Company, and P. A. Andrekson, “Overcoming the quantum limit of optical amplification in monolithic waveguides,” *Sci. Adv.*, vol. 7, no. 38, pp. 8150–8165, 2021.

[5] B. Shen *et al.*, “Integrated turnkey soliton microcombs,” *Nature*, vol. 582, no. 7812, pp. 365–369, 2020.

[6] J. Wang, F. Sciarrino, A. Laing, and M. G. Thompson, “Integrated photonic quantum technologies,” *Nature Photonics*, vol. 14, no. 5. pp. 273–284, 2020.

[7] W. Bogaerts *et al.*, “Programmable photonic circuits,” *Nature*, vol. 586, no. 7828. pp. 207–216, 2020.

[8] C. R. Pollock and M. Lipson, *Integrated photonics*, 2003.

[9] S. Roberts, X. Ji, J. Cardenas, M. Corato-Zanarella, and M. Lipson, “Measurements and modeling of atomic-scale sidewall roughness and losses in integrated photonic devices,” *arXiv Prepr. arXiv2105.11477*, 2021.

[10] N. Bai, X. Zhu, Y. Zhu, W. Hong, and X. Sun, “Tri-layer gradient and polarization-selective vertical couplers for interlayer transition,” *Opt. Express*, vol. 28, no. 15, p. 23048, 2020.

[11] W. D. Sacher, Y. Huang, G. Q. Lo, and J. K. S. Poon, “Multilayer silicon nitride-on-silicon integrated photonic platforms and devices,” *J. Light. Technol.*, vol. 33, no. 4, pp. 901–910, 2015.

[12] W. D. Sacher *et al.*, “Tri-layer silicon nitride-on-silicon photonic platform for ultra-low-loss crossings and interlayer transitions,” *Opt. Express*, vol. 25, no. 25, p. 30862, 2017.

[13] Z. Ye, K. Twayana, P. A. Andrekson, and V. Torres-Company, “High-Q Si3N4 microresonators based on a subtractive processing for Kerr nonlinear optics,” *Opt. Express*, vol. 27, no. 24, pp. 35719–35727, 2019.

[14] K. Twayana, Z. Ye, Ó. B. Helgason, K. Vijayan, M. Karlsson, and V. Torres-Company, “Frequency-comb-calibrated swept-wavelength interferometry,” *Opt. Express*, vol. 29, no. 15, p. 24363, 2021.

[15] D. Melati, A. Melloni, and F. Morichetti, “Real photonic waveguides: guiding light through imperfections,” *Adv. Opt. Photonics*, vol. 6, no. 2, p. 156, 2014.